

Supplementary Materials and Methods

Patients and samples. Samples from 378 donors (shown in Sup. Table 6) were obtained from central-south region of China, including Wuhan Brain Hospital and Xiangya Hospital during surgical resection between 2011 and 2016. Tissue samples were collected during surgery and rapidly transferred to the laboratory on wet ice. A portion of each tissue sample was fixed with 4% paraformaldehyde and the remainder was divided into 10 aliquots in 2ml freezing tubes (20mg/tube), then immediately frozen in liquid nitrogen. Two blood samples were collected from each subject, one with anticoagulant and the other without anticoagulant, and transferred to the laboratory on wet ice for DNA extraction and serum separation, respectively. There were 215 samples from glioma patients (143 HGG and 72 LGG); an additional 117 samples were non-glioma brain tumors, including meningioma, neurinoma, acoustic neuroma, craniopharyngioma, neuroinomatosis, hypophysoma, and cavernous hemangioma; 24 samples were from patients with non-tumor brain diseases, including epilepsy, gliosis, and Burner's disease, and 22 were from normal brain tissues obtained during surgery on patients with cerebral trauma or cerebral hemorrhage. Tumor locations included the frontal, parietal, temporal, occipital lobe and cerebellum. All brain tumors were independently histologically diagnosed and verified according to the WHO Classification of Tumors of the Central Nervous System (2007) (Louis et al., 2007) by two neuropathologists who were blinded to the clinical data. All tumor patients received standard postoperative treatment with radiation and chemotherapy.

Paired peripheral blood and brain tissue samples were collected from 145 of the

glioma patients and survival information was available from 84 glioma patients. Among the 84 glioma patients, paraffin-embedded brain tissues, frozen tissues, and paired blood samples were available from 36 patients, while for the remaining 48 cases only paraffin-embedded brain tissues were available.

Serology examination. HCMV-specific IgG and IgM were determined by the Affiliated Shengjing Hospital of China Medical University, Shenyang, as described previously (Wen et al., 2017). Chemiluminescent immunoassay methods were applied using an automatic LIAISON analyzer XL (Diasorin S.P.A., Italy) with appropriate LIAISON CLIA kits (HCMV IgG Cat.#310760, HCMV IgM Cat.#310756) on an automated LIAISON analyzer XL (DiasorinS.p.A., Italy) following the manufacturer's instructions. Sera were scored as seropositive or seronegative based on cut-off values provided by the manual.

Viral DNA detection. Brain tissues and whole blood were tested for the presence of DNA from nine human herpesviruses using nested PCR as previously described (Wen et al., 2017). Briefly, total DNA was extracted from 20 mg of fresh brain tissue or 500 μ l whole blood with using a TIANamp Genome DNA Kit (TIANGEN Biotech, China) following the manufacturer's instructions. DNA samples were divided into five aliquots and stored at -80 °C. The first round of PCR amplification used 500 ng of DNA (quantitated by a NANODROP2000 Spectrophotometer, Thermo Fischer Scientific, USA) as template. The second round of PCR used two μ l of the first round reaction as template and inner primer pairs. Second round PCR reactions were separated by agarose gel electrophoreses, stained with SYBR Safe DNA gel stain, and

imaged using a Gel Doc XR+ Gel Documentation System (Bio-Rad, USA). Reactions with clearly visible PCR products were confirmed as having an appropriate size by comparison to positive controls.

Droplet digital PCR was conducted using primers and probe specific to HCMV *UL83* gene sequences using a QX200 system (Bio-Rad, USA) according to the manufacturer's instructions as previously described (Luo, Li, Yang, Yu, & Wei, 2017). Briefly, 22 μ l reaction mixtures consisting of 1x Supermix (Bio-Rad, USA), 0.25 μ M of probe, 0.9 μ M of each primer, and 500 ng of DNA extracted from brain tissues were partitioned into nanoliter-sized droplets using an automated droplet generator (Bio-Rad, USA). After heat-sealing in 96-well plates with pierceable foil using a PX1 PCR plate sealer (Bio-Rad, USA), reactions were amplified in a conventional thermal cycler (C100 Touch, Bio-Rad) and fluorescence in each well was measured using a Q200 droplet reader (Bio-Rad, USA). The data of positive and negative droplets obtained were analyzed using the software package provided (QuantaSoft, Bio-Rad, USA). Assays for which total droplet counts were below 10,000 were excluded. All primer pairs were listed in Sup. Table. 7

Viruses and virus infection. Positive controls of nine herpesviruses for nested PCR were HSV1 strain H129 (Zeng et al., 2017), HSV2 strain G (kindly given by Prof. Qinxue Hu, WHIOV, CAS, China), VZV strain Oka (H. F. Jiang et al., 2017), EBV-positive cell line B95.8 (kindly given by Prof. Ya Cao, Central South University, Changsha, China) (S. F. Liu, Li, Tang, & Cao, 2018), plasmid of pUC8 containing a DNA fragment of HHV-6A strain U1102 (Lawrence et al., 1990), plasmid pMD18-T

containing a DNA fragment of HHV7 strain RK (kindly given by Dr. Meei-Li Huang, University of Washington, Seattle, USA), and KSHV-Bac36 (kindly given by Prof. Shou-Jiang Gao, UPMC Hillman Cancer Center, University of Pittsburgh, Pittsburgh, USA)(Peng, Chen, Tang, Liu, & Chen, 2014). HCMV TB40E was kindly provided by Prof. Hua Zhu, Rutgers New Jersey Medical School, New Jersey, USA. Human embryo lung fibroblasts (HELs) grown on coverslips (1×10^5 /10-mm cover slip) were infected with HCMV strain Towne (ATCC-VR977) (Pan et al., 2013) at a MOI=1. 72 hours post infection cells were fixed and target proteins were detected by IHC as described below.

Histological staining and evaluation. Brain tissue samples were fixed with 4% paraformaldehyde, and embedded in paraffin. H&E staining was performed following a standard protocol (Jin et al., 2011). Brain tissues embedded in paraffin were cut into 4- μ m-thick sections. Briefly, the sections were then deparaffinized in xylene, rehydrated in a graded series of alcohol *to* water. Slides were stained with Harris hematoxylin solution for 5 min and differentiated in acid alcohol for 10 s. After rinsing in running tap water for 15 min, the sections were then stained in eosin solution for 1 min, dehydrated in alcohol, cleared in xylene and mounted with coverslips.

HCMV proteins IE1/2, pp65, and gB were detected by a two-step-visualization (Dextran-based polymer method) immunohistochemistry (IHC) staining following a modified protocol described previously (Cobbs et al., 2002). 6- μ m-thick brain tissues sections were deparaffinated conventionally and were immersed with 3% H₂O₂ for 10

min to block endogenous peroxidase. After antigen retrieval by microwave, new-born calf serum was added for blocking for 10 min, and then the primary antibody was added to incubate overnight (4 °C). Secondary antibodies were incubated and signals were visualized with 3,30-diaminobenzidine (DAB) (Cat. #KIHC-5, Proteintech, China). After hematoxylin staining, dehydration and hyalinization, the slips were covered. For the negative control, primary antibodies or secondary antibodies were replaced by phosphate buffered saline (PBS). Images were obtained using a Chirascan-SF digital slice scanning system (Thermo Fischer Scientific, USA).

To determine viral protein expression levels, images of all sections were independently and blindly evaluated by two investigators. Yellow- or brown-stained areas in nuclei or cytoplasm were considered positive signals and the IOD of the staining was measured in all five random fields per section using Image-Pro Plus 6.0 (Media Cybernetics Inc., USA) through batch scanning.

IHC results were evaluated using a modified scoring methodology described previously (Wang et al., 2017). In brief, IHC-stained samples with positive cell percentages of >50%, 26-50%, 5-25%, or <5% were scored as +++, ++, +, or -, respectively, as previously reported (Rahbar et al., 2012). Signals of dark-brown, light-brown, light-yellow, or light-blue (hematoxylin only) were scored as +++, ++, +, or -, respectively.

Isolation of primary glioma cells. Primary glioma cells were isolated from fresh tumor tissues as described previously (Clark et al., 2017). Briefly, the tumor tissues were resected during surgery, maintained on wet ice in HBSS (Cat.#14025-076, Life

Technology, USA), and delivered to the laboratory within 5 hours. After rinsing with HBSS the tissues were minced into small pieces, digested using collagenase (Sigma, USA) and DNase I (Roche, Germany) at 37 °C for 30 min., ground gently with a rubber 5 cc syringe plunger, and filtered through 70 µm nylon filters. Red blood cells were removed with RBC Lysis Buffer (Cat.#420301, Biolegend, USA) and remaining cells were divided into two aliquots and pelleted by centrifugation. One aliquot was used for monolayer culture, which was suspended in DMEM/F12 (Cat. #11320-033, Life Technology) supplemented with 10% fetal bovine serum (FBS), 1% penicillin-streptomycin (100U/ml and 100µg/ml), and 4 mM L-glutamine. The other was used for sphere culture, which was suspended in DMEM/F12 (Cat. #11320-033, Life Technology) supplemented with 1% penicillin-streptomycin (100U/ml and 100µg/ml), 20ng/ml bFGF (Cat. #cyt-218-c, Prospec), 20 ng/ml EGF (Cat. #cyt-217-c, Prospec), 10% BIT9500 (Cat. #09500, Stemcell Technologies), 2µg/ml amphotericin B (Cat.#A2942,Sigma), 50µg/ml gentamicin (Cat. #15750-060, Life Technology), 2% B27 (Cat. #12587010), and 1% GlutaMAX (Cat.#35050-061, Life Technology). Cells were cultured as described previously (X. J. Liu et al., 2017; Wang et al., 2017) and serial subcultures were maintained within 4-6 passage.

Immunofluorescence analysis (IFA). Primary glioma cells and glioma stem-like cells were seeded onto coverslips and fixed with 4% paraformaldehyde after attachment. HELs were grown on coverslips and were either not infected, mock infected, or virus infected at an MOI of 1. After permeabilization as described previously (Duan et al., 2012), IE1/2 proteins were detected and nuclei were

counterstained with DAPI (Cat. #D9542, Sigma). Images were obtained using the Fusion Shell software tool on a High Speed Confocal scanning microscope (Dragonfly 200, ANDOR).

Lentivirus propagation and transduction. HEK293T(ATCC, CRL-321) and Human glioblastoma cell lines U118(ATCC® HTB-15), U251 (purchased from the Shanghai Institute of Cell Biology, Chinese Academy of Sciences), A172 (ATCC® CRL-1620™), and LN229 (ATCC® CRL-2611™) were cultured in DMEM(Gibco/Life Technology) supplemented with 10% fetal bovine serum (Gibco/Life Technology) and penicillin-streptomycin (100 U/ml and 100 µg/ml). Cells were maintained at 37 °C in a humidified atmosphere containing 5% CO₂.Lentivirus vectors based on the pHAGE-CMV-MCS-IZsGreen system (referred as pHAGE) (X. J. Liu et al., 2017), kindly provided by Prof. Chaoyang Li (WHIOV, CAS, China), were constructed to transduce cells to express HCMV IE1 or IE2 proteins. The cDNA sequences for IE1 and IE2 were cloned into pHAGE to generate plasmids pHAGE-IE1 and pHAGE-IE2, respectively. Plasmids pHAGE-IE1, pHAGE-IE2, or pHAGE were transfected into HEK293T cells along with helper plasmids pSPAX and pMD2G (X. Jiang et al., 2018) to produce lentivirusesLV-IE1, LV-IE2, and LV-Ctl, respectively. Glioma cells were transduced with the lentiviruses and transduction efficiency was monitored by GFP fluorescence and IE1 and IE2 protein levels. The latter were determined by western blotting when GFP was observed in over 90% of the cells.

Western blotting. Cells were harvested and lysed with cell lysis buffer (Cat. #P0013,

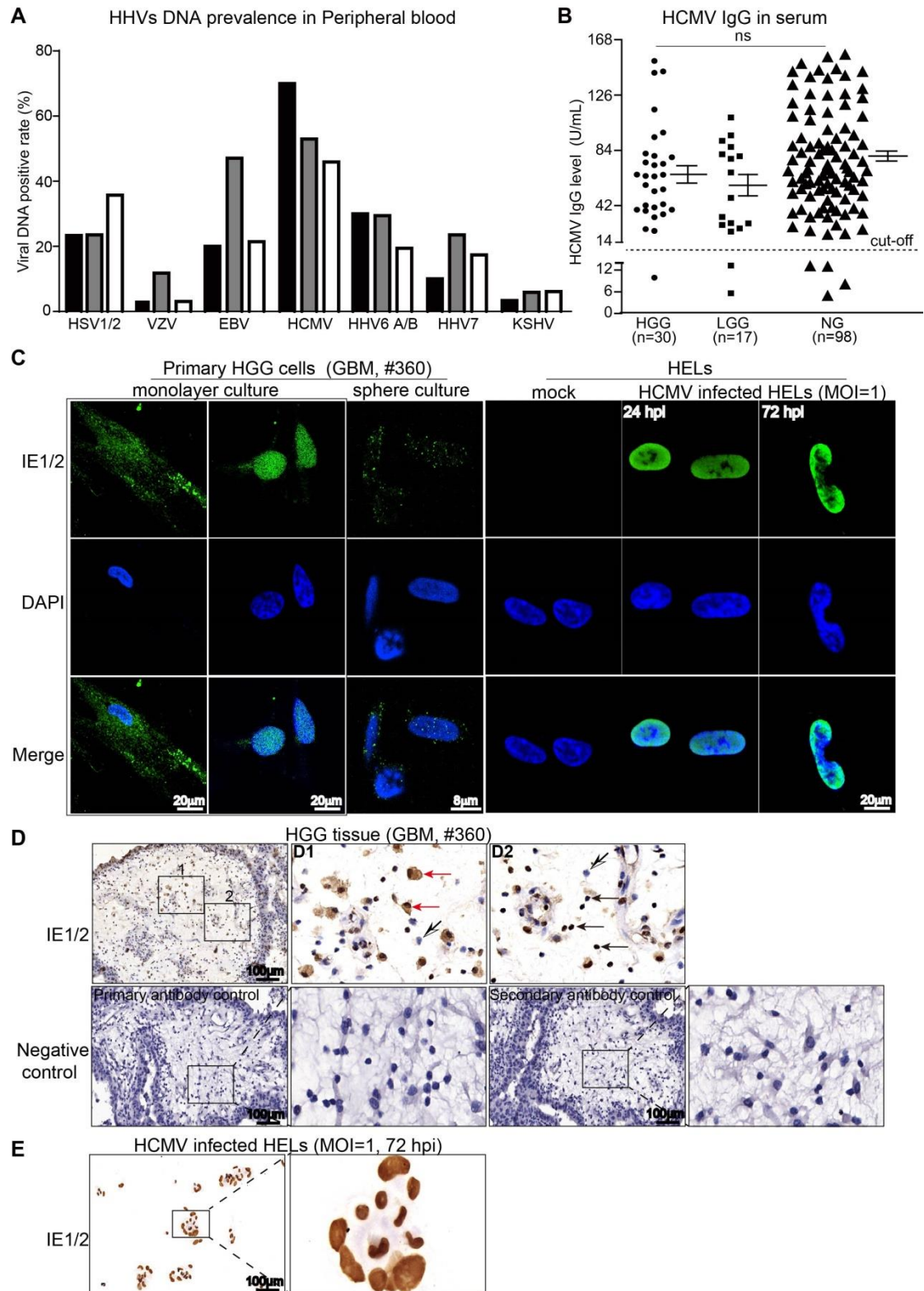
Beyotime) containing protease inhibitor cocktail (Cat. #04693159001, Roche), as recommended by the manufacturer. Protein concentrations were determined by Bradford assay (Cat. #500-0205, Bio-Rad). Cell lysates with equal amounts of total protein were separated by SDS-polyacrylamide gel electrophoresis and transferred to polyvinylidenedifluoride membranes (Cat. #ISEQ00010, Millipore). Membranes were sequentially probed with primary antibodies and appropriate peroxidase-conjugated secondary antibodies, developed using SuperSignal West Femtochemiluminescent substrate (Cat. #34095, Life Technologies), and visualized using a FluorChem HD2 system (Alpha Innotech). GAPDH served as a loading control. All the antibodies used in the study were listed in Sup. Table 8.

Evaluation of cell proliferation and migration. Cell proliferation was evaluated by MTT assay (Cat.#M2128-1G, Sigma, USA) following the manufacturer's instructions. Briefly, cells were seeded in 96-well plates at a density of 5×10^3 cells/well with eight replicates. After culture for 48 h the cells were incubated with MTT for 4 h at 37 °C, then lysed in 150 µl dimethyl sulfoxide (DMSO). Optical absorbance was measured at 490 nm using a microplate reader (Synergy HT, BioTek, USA). Relative proliferation was calculated as the ratios of MTT optical absorbance values for LV-IE1- or LV-IE2-transduced cells to those of corresponding LV-Ctl-transduced control cells.

Cell migration assays were performed using a transwell system. 5.0×10^4 cells in 100 µl serum-free culture medium (DMEM for glioma cell lines and DMEM/F12 for primary glioma cells) were seeded into the top chambers of 24-well transwell plates and 600 µl of matching medium containing 10% fetal bovine serum was added to the

lower chambers. Following incubation at 37°C for 24 h the remaining cells that had not migrated from the top of the membrane were removed using a cotton-tipped applicator. Cells on the lower surface were then fixed in 4% paraformaldehyde and stained with 1% crystal violet. Five random fields of the lower surface were imaged and cells were manually counted using Image-Pro Plus 6.0 (Media Cybernetics, USA).

Statistical analyses. Differences in DNA prevalence between different groups were analyzed using Chi-square test and performed in R (Team, 2016). HCMV viral loads among different groups were analyzed by the Kruskal-Wallis-Test. Correlations between protein levels (defined according to protein level scores), patient characteristics and, survival time were analyzed with Cox regression and Kaplan–Meier curves. Survival analyses between two groups of patients with high or low protein levels were performed by log-rank test. Differences in HCMV protein expression based on IHC between glioma and non-glioma or between HGG and LGG patients were analyzed by one-way ANOVA. Cell proliferation and migration data were analyzed by Student's t-test. Statistical analyses were conducted using the SPSS Statistics 17.0 software (IBM, New York, USA). Differences were considered statistically significant at P values of ≤ 0.05 .



Supplementary Figure legend

Sup. Figure 1. Subcellular localization of IE1/2 proteins in HGG tissues and primary cells. (A) Paired samples from 145 subjects with high-grade glioma (HGG),

low-grade glioma (LGG), or non-glioma (NG) were analyzed by nested PCR to detect the presence of HHVs DNA in peripheral blood. (B) HCMV-specific serum IgG levels were determined using the DiaSorin LIAISON® immunoassay system; samples below the cut-off (dotted line) are considered negative. (C) Subcellular localization of IE1/2 in primary glioma cells (monolayer culture) and glioma stem-like cells (sphere culture) determined by IFA. Cells were derived from HGG tissue of GBM case #360. Mock- and HCMV-infected HELs were used as negative and positive controls, respectively. HELs grown on coverslips were mock- or HCMV-infected at an MOI of 1, and coverslips were collected at 24 and 72 hours post infection (hpi). (D) Subcellular localization for IE1/2 proteins in HGG tissue of GBM case #360 determined by IHC staining. Open arrows indicate IE1/2-negative cells (D1 and D2); black arrows indicate cells with exclusively nuclear localization of IE1/2 proteins (D1); red arrows indicate cells with both nuclear and cytoplasmic localization of IE1/2 proteins (D2). Primary and secondary antibodies controls are shown in the lower panel. (E) Localization of IE1/2 proteins detected by IHC staining of fibroblasts infected with HCMV strain Towne at an MOI of 1 at 72 h post infection.

Supplementary Tables

Sup. Table 1. Logistic regression model used to analyse the association between HCMV protein levels (IE1/2, pp65 and gB), patients characteristics and tumor grade

Sup. Table 1-1. IE1/2

Model	Df	Resid. Df	Resid. Df	Resid. Dev	P value
Tumor_grade + Tumor_location +Sex +Age	1	2.469	105	135.96	0.116
Tumor_grade + Tumor_location +Sex	1	1.741	106	138.43	0.187
Tumor_grade + Tumor_location	2	3.752	107	140.17	0.153
Tumor_grade	1	8.435	109	143.92	0.004

	Estimate	Std. Error	z value	Pr(> z)
(Intercept)	-.0606	0.359	-1.689	0.0912 .
Tumor_grade A	1.222	0.431	2.836	0.0046 **

Odds ratio	95%CI
3.395062	(1.481477, 8.104861)

Sup. Table 1-2. pp65

Model	Df	Resid. Df	Resid. Df	Resid. Dev	P value
Tumor_grade + Tumor_location +Sex +Age	1	1.138	105	131.83	0.286
Tumor_grade + Tumor_location +Sex	1	0.004	106	132.97	0.951
Tumor_grade + Tumor_location	2	0.204	107	132.98	0.903
Tumor_grade	1	6.699	109	133.18	0.010

	Estimate	Std. Error	z value	Pr(> z)
(Intercept)	1.767e-15	3.430e-01	0.000	1.000
Tumor_grade A	1.116e+00	4.330e-01	2.577	0.010 **

Odds ratio	95%CI
3.052632	(1.311861, 7.22309)

Sup. Table 1-3. gB

Model	Df	Resid. Df	Resid. Df	Resid. Dev	P value
Tumor_grade + Tumor_location +Sex +Age	1	0.024	105	146.23	0.878
Tumor_grade + Tumor_location +Sex	1	1.679	106	146.25	0.195
Tumor_grade + Tumor_location	2	1.608	107	147.93	0.448
Tumor_grade	1	2.815	109	149.54	0.093

	Estimate	Std. Error	z value	Pr(> z)
(Intercept)	-0.7376	0.3666	-2.012	0.044 *
Tumor_grade A	0.7116	0.4317	1.649	0.100 .

Odds ratio	95%CI
2.037296	(1.013882, 4.223268)

Sup.Table 2. Categorical Variable Codings^b used in Kaplan-Meier curves shown in Fig. 1F

	n	mean	Std. Error	95% CI from mean	-1	-2	-3
group IE1/2_grade ^a	84	32.167	5.123	(22.126-42.208)			
1=group: group IE1/2=0 ^c and grade=0 ^d	9	35.000	3.490	(28.160-41.840)	0.75	-0.25	-0.25
2=group: group IE1/2=1 and grade=0	6	47.220	7.629	(32.267-62.173)	-0.25	0.75	-0.25
3=group: group IE1/2=0and grade=1	18	19.733	2.539	(14.757-24.709)	-0.25	-0.25	0.75
4=group: group IE1/2=1 and grade=1	51	28.443	3.193	(22.185-34.700)	-0.25	-0.25	-0.25

a. Simple Parameter Coding

b. Category variable: group IE1/2* grade (group IE1/2_grade)

c. IE1/2^{low}: 0; IE1/2^{high}: 1

d. Tumor grade: High-grade glioma =1, Low-grade glioma =0

Chi-square=15.681, P=0.028

Sup.Table 3. Variables used in the Cox regression analysis to consider association between patient prognosis and HCMV protein/patient characteristics

	B	SE	Wald	P	Exp (B)	95% CI for Exp (B)	
						Lower	Upper
IE1/2 *grade			13.230	.004			
IE1/2 *grade (1)	-1.397	.642	4.739	.029	.247	.070	.870
IE1/2 *grade (2)	-1.129	.617	3.351	.067	.323	.096	1.083
IE1/2 *grade (3)	-1.532	.545	8.198	.004	.210	.072	.611
pp65	-.423	.351	1.450	.228	.655	.329	1.304
gB	-.400	.350	1.302	.254	.671	.338	1.332
gender	-.127	.319	.159	.690	.881	.471	1.645
age	-.353	.507	.485	.486	1.423	.527	3.842

grade: tumor grade

Chi-square=11.557, P=0.009

Sup.Table 4. Assigned coefficients of variables in the Cox Regression analysis in Fig.1F

	B	SE	Wald	P	OR	95% CI for OR	
						Lower	Upper
group IE1/2 * grade			10.334	.016			
group IE1/2 * grade (1)	-1.107	.605	3.349	.067	.330	.101	1.082
group IE1/2 * grade (2)	-.974	.608	2.572	.109	.337	.115	1.242
group IE1/2 * grade (3)	-1.318	.529	6.214	.013	.268	.095	.754

Sup.Table 5. Ki67 levels in HGG and LGG tissues based on IHC staining^a

Ki67 levels	+++	++	+	-	P value
	No. (%)	No. (%)	No. (%)	No. (%)	
HGG (n=78)	40 (51.3%)	28 (35.9%)	8 (10.3%)	2 (2.6%)	<0.01
LGG (n=30)	0	2 (14.3%)	2 (14.3%)	8 (35.7%)	

^aScores based on IHC scoring (Sup. Materials and Methods) from five random fields per specimen. Data were analyzed by chi-square test.

Sup.Table 6. Characteristics of patients in the study

Category	Diseases	n	Gender (Female/Male)	Adults		Children	
				n	Age Mean (range)	n	Age Mean (range)
HGG	Grade IV (GBM)	64	22/42	44	48 (14-74)	20	6 (2-13)
	Grade III	80	35/45	76	49 (15-79)	4	7 (2-10)
LGG	Grade II	66	33/33	59	44 (15-72)	7	6 (2-10)
	Grade I	5	1/4	4	34 (25-43)	1	3
	Other brain tumor	117	75/42	111	52 (19-78)	6	8 (2-12)
NG	Non-tumor brain disease	24	8/16	12	26 (15-51)	12	5 (1-12)
	Normal brain tissue	22	10/12	18	55 (20-75)	4	5 (1-12)
Totals		378	184/194	324	49 (14-79)	54	6 (1-13)

Sup.Table 7. PCR Primers used for detection of viral DNAs

Assay	Virus	Gene	Primer	Sequence (5'-3')	Product size (bp)
Nested PCR	HSV 1/2	UL30	outer F	TGCTCATCAAGGGCGTGGATCTGG	456
			outer R	CTGGGGCGGCGGCGTCTAG	
			inner F	GACTTTGTCTCACCGCCGAAC TG	178
			inner R	GCGCGACCGTCTCCTCTACCTC	
	EBV	LMP1	outer F	GCCCTCCTTGTCCTCTATTCTT	1080 ^a
			outer R	TCATCATCTCCACCGGAACCAG	/1125
			inner F	GCTGTTCATCTTCGGGTGCTT	270
			inner R	GGAGCCAAAGGAGATCAACCAA	
	HCMV	UL83	outer F	GACGCGTCAGCAGAACCAGTGGAAA	1058
			outer R	AGATGTCGTTGGCGTCCCAGAAGAA	
			inner F	TTTACCTCACACGAGCATTTTGGGC	527
			inner R	TCCTCGTCGGTGTCTCTT	
	VZV	ORF62	outer F	CGGTCACCCTTCTCCAACAAC	1857
			outer R	GCCACCGACACGATGCTCA	
			inner F	CCCCGTGAATACCGGCAGT	419
			inner R	CTCCCCTCCAACACCGTCTC	
	HHV6 A/B	U64	outer F	GTTGGTACGAGCTTTCGTTTTCCCG	269
			outer R	AATCCAAAAATCTTCCCGAGCTGC	
			inner F	GAGAATAATTTACTGTCCGCTTCCC	142
			inner R	ATTGCCATTATGAATCTGAAGCGT	
HHV7	U10	outer F	TATCCCAGCTGTTTTCATATAGTAAC	186	
		outer R	GCCTTGCGGTAGCACTAGATTTTTTG		
		inner F	CAGAAATGATAGACAGATGTTGG	124	
		inner R	TAGATTTTTTGAAAAAGATTAATAAC		
KSHV	ORF50	outer F	TGGAAAGCTTCGTCGGCCTC	935	
		outer R	CCACGTAATAAACGCCGGGTC		
		inner F	CTGAAGGCCCAACTCTACCAG	292	
		inner R	TGCAGAATAAGATCCTCTCCGTGA		
Digital dropletPCR	HCMV	UL83	F	ACGCAAATCAGCATCCTC	124
R	GTGGATTCGTTGTCGGA				
probe	TCCTCGTCGGTGTCTCTTCG				

^a The size of PCR products may vary according to the strain polymorphism of EBV in subjects.

Sup.Table 8. Antibodies used in the study

Antibody (clone)	Species / Isotype	Source / Cat#
Primary antibody		
Anti-IE1 (clone IE1.G10)	Mouse monoclonal/IgG ₁	Abcam/ab30924
Anti-IE2 (clone 12E2)	Mouse monoclonal/IgG ₁	Santa Cruse/SC-69835
Anti-IE1/2 (clone CH16)	Mouse monoclonal/IgG ₁	Virusys/P1215
Anti-pp65 (clone CH12)	Mouse monoclonal/IgG ₁	Virusys/P1205
Anti-gB (clone CH28)	Mouse monoclonal/IgG ₁	Virusys/ P1201
Anti-Ki67	Rabbit polyclonal	Abcam/ab15580
Second antibody		
Alexa Fluor 488-conjugated goat anti-mouse IgG1	Goat	Invitrogen/A-21121
Peroxidase-anti-Mouse IgG	Goat	Jackson ImmunoResearch Laboratories/115-035-003
Peroxidase-anti-Rabbit IgG	Goat	Jackson ImmunoResearch Laboratories/111-035-003

- Clark, P. A., Bhattacharya, S., Elmayan, A., Darjatmoko, S. R., Thuro, B. A., Yan, M. B., . . . Kuo, J. S. (2017). Resveratrol targeting of AKT and p53 in glioblastoma and glioblastoma stem-like cells to suppress growth and infiltration. *Journal of Neurosurgery*, *126*(5), 1448-1460. doi:10.3171/2016.1.Jns152077
- Cobbs, C. S., Harkins, L., Samanta, M., Gillespie, G. Y., Bharara, S., King, P. H., . . . Britt, W. J. (2002). Human cytomegalovirus infection and expression in human malignant glioma. *Cancer Res*, *62*(12), 3347-3350.
- Duan, Y. L., Miao, L. F., Ye, H. Q., Yang, C. Q., Fu, B. S., Schwartz, P. H., . . . Luo, M. H. (2012). A faster immunofluorescence assay for tracking infection progress of human cytomegalovirus. *Acta Biochimica Et Biophysica Sinica*, *44*(7), 597-605. doi:10.1093/abbs/gms041
- Jiang, H. F., Wang, W., Jiang, X., Zeng, W. B., Shen, Z. Z., Song, Y. G., . . . Luo, M. H. (2017). ORF7 of Varicella-Zoster Virus Is Required for Viral Cytoplasmic Envelopment in Differentiated Neuronal Cells. *Journal of Virology*, *91*(12). doi:UNSP e00127-17
10.1128/JVI.00127-17
- Jiang, X., Dong, X., Li, S. H., Zhou, Y. P., Rayner, S., Xia, H. M., . . . Luo, M. H. (2018). Proteomic Analysis of Zika Virus Infected Primary Human Fetal Neural Progenitors Suggests a Role for Doublecortin in the Pathological Consequences of Infection in the Cortex. *Frontiers in Microbiology*, *9*. doi:ARTN 1067
10.3389/fmicb.2018.01067
- Jin, F., Gao, C., Zhao, L., Zhang, H., Wang, H. T., Shao, T., . . . Zhao, H. Y. (2011). Using CD133 positive U251 glioblastoma stem cells to establish nude mice model of transplanted tumor. *Brain Res*, *1368*, 82-90. doi:10.1016/j.brainres.2010.10.051
- Lawrence, G. L., Chee, M., Craxton, M. A., Gompels, U. A., Honess, R. W., & Barrell, B. G. (1990). Human herpesvirus 6 is closely related to human cytomegalovirus. *J Virol*, *64*(1), 287-299.
- Liu, S. F., Li, H. D., Tang, M., & Cao, Y. (2018). (-)-Epigallocatechin-3-gallate inhibition of Epstein-Barr virus spontaneous lytic infection involves downregulation of latent membrane protein 1. *Experimental and Therapeutic Medicine*, *15*(1), 1105-1112. doi:10.3892/etm.2017.5495
- Liu, X. J., Yang, B., Huang, S. N., Wu, C. C., Li, X. J., Cheng, S., . . . Luo, M. H. (2017). Human cytomegalovirus IE1 downregulates Hes1 in neural progenitor cells as a potential E3 ubiquitin ligase. *Plos Pathogens*, *13*(7).
- Louis, D. N., Ohgaki, H., Wiestler, O. D., Cavenee, W. K., Burger, P. C., Jouvett, A., . . . Kleihues, P. (2007). The 2007 WHO classification of tumours of the central nervous system (vol 114, pg 97, 2007). *Acta Neuropathologica*, *114*(5), 547-547.
- Luo, J., Li, J. H., Yang, H., Yu, J. P., & Wei, H. P. (2017). Accurate Detection of Methicillin-Resistant

Staphylococcus aureus in Mixtures by Use of Single-Bacterium Duplex Droplet Digital PCR. *Journal of Clinical Microbiology*, 55(10), 2946-2955.

Pan, X., Li, X. J., Liu, X. J., Yuan, H., Li, J. F., Duan, Y. L., . . . Luo, M. H. (2013). Later Passages of Neural Progenitor Cells from Neonatal Brain Are More Permissive for Human Cytomegalovirus Infection. *Journal of Virology*, 87(20), 10968-10979. doi:10.1128/Jvi.01120-13

Peng, C., Chen, J. G., Tang, W., Liu, C. L., & Chen, X. L. (2014). Kaposi's Sarcoma-Associated Herpesvirus ORF6 Gene Is Essential in Viral Lytic Replication. *Plos One*, 9(6). doi:ARTN e99542
10.1371/journal.pone.0099542

Rahbar, A., Stragliotto, G., Orrego, A., Peredo, I., Taher, C., Willems, J., & Soderberg-Naucler, C. (2012). Low levels of Human Cytomegalovirus Infection in Glioblastoma multiforme associates with patient survival; -a case-control study. *Herpesviridae*, 3, 3. doi:10.1186/2042-4280-3-3

Team, R. C. (2016). A language and environment for statistical computing. Retrieved from <https://www.R-project.org/>

Wang, X., Wang, Y., Liu, D., Wang, P., Fan, D., Guan, Y., . . . An, J. (2017). Elevated expression of EBV and TLRs in the brain is associated with Rasmussen's encephalitis. *Virology*, 512(2), 423-430. doi:10.1016/j.virus.2017.04.008

Wen, L., Qiu, Y., Cheng, S., Jiang, X., Ma, Y. P., Fang, W., . . . Luo, M. H. (2017). Serologic and viral genome prevalence of HSV, EBV, and HCMV among healthy adults in Wuhan, China. *J Med Virol*. doi:10.1002/jmv.24989

Zeng, W. B., Jiang, H. F., Gang, Y. D., Song, Y. G., Shen, Z. Z., Yang, H., . . . Luo, M. H. (2017). Anterograde monosynaptic transneuronal tracers derived from herpes simplex virus 1 strain H129. *Molecular Neurodegeneration*, 12. doi:ARTN 38
10.1186/s13024-017-0179-7